Mon. Not. R. Astron. Soc. 000, 1–12 (2010) Printed 5 June 2012 (MN LATEX style file v2.2)

Star formation in HI tails: HCG 92, HCG 100 and 6 interacting systems*

D. F. de Mello[1,2]†, F. Urrutia-Viscarra[3], C. Mendes de Oliveira[3], S. Torres-Flores[4], E. R. Carrasco[5], E. Cypriano [3]

[1] The Catholic University of America, Physics Department, Washington, DC 20064, USA
[2] Observational Cosmology Laboratory, Code 665, Goddard Space Flight Center, Greenbelt, MD 20771, USA
[3] Departamento de Astronomia, Instituto de Astronomia, Geofísica e Ciências Atmosféricas da USP, Rua do Matão 1226, Cidade Universitária, 05508-090, São Paulo, Brazil
[4] Departamento de Física, Universidad de La Serena, Av. Cisternas 1200 Norte, La Serena, Chile
[5] Gemini Observatory/AURA, Southern Operations Center, Casilla 603, La Serena, Chile

ABSTRACT

We present new Gemini spectra of 14 new objects found within the HI tails of Hickson Compact Groups 92 and 100. Nine of them are GALEX Far-UV (FUV) and Near-UV (NUV) sources. The spectra confirm that these objects are members of the compact groups and have metallicities close to solar, with an average value of 12+log(O/H)~8.5. They have average FUV luminosities 7×10^{40} erg s^{-1}, very young ages (< 100 Myr) and two of them resemble tidal dwarf galaxies (TDGs) candidates. We suggest that they were created within gas clouds that were ejected during galaxy-galaxy interactions into the intergalactic medium, which would explain the high metallicities of the objects, inherited from the parent galaxies from which the gas originated. We conduct a search for similar objects in 6 interacting systems with extended HI tails, NGC 2623, NGC 3079, NGC 3359, NGC 3627, NGC 3718, NGC 4656. We found 35 UV sources with ages < 100 Myr, however most of them are on average less luminous/massive than the UV sources found around HCG 92 and 100. We speculate that this might be an environmental effect and that compact groups of galaxies are more favorable to TDG formation than other interacting systems.

Key words: galaxies: interactions – galaxies: star formation – (galaxies:) intergalactic medium – galaxies: star clusters

1 INTRODUCTION

Interacting galaxies are ideal laboratories to probe galaxy evolution since tidal interaction is an important mechanism in shaping galaxies properties as we measure today. The HI gas, which is both the reservoir for star formation and an excellent tracer of the large-scale galaxy dynamics, is affected by tidal interaction and is often found in tails outside interacting galaxies. One of the key questions regarding the encounters of disk galaxies is the fate of the stripped HI gas. Do these HI intergalactic clouds form new stellar systems and/or dwarf galaxies known as tidal dwarf galaxies (TDGs)? And if they do, is there any difference in the types of objects that could be formed based on the type of environment where they are located? We have embarked in a series of papers trying to answer theses questions. In Torres-Flores et al. (2009), de Mello et al. (2008a) and Mendes de Oliveira et al. (2004, 2006) we showed a few Hickson Compact Groups (HCGs) contain TDGs and intragroup star-forming regions. Other authors have also found **TDGs** and many young globular cluster candidates in compact groups (e.g., Iglesias-Páramo & Vílchez 2001 and Gallagher et al. 2001). Other cases of intergalactic star-forming regions have also been reported outside interacting galaxies (e.g. Ryan-Weber et al. 2004, Mullan et al. 2011, Oosterloo et al. 2004, Werk et al. 2011), including young (<10 Myr) small stellar clusters in the HI bridge between M81 and M82 (de Mello

* Based on observations obtained at the Gemini Observatory, which is operated by the Association of Universities for Research in Astronomy, Inc., under a cooperative agreement with the NSF on behalf of the Gemini partnership: the National Science Foundation (United States), the Science and Technology Facilities Council (United Kingdom), the National Research Council (Canada), CONICYT (Chile), the Australian Research Council (Australia), Ministério da Ciência e Tecnologia (Brazil), and Ministerio de Ciencia, Tecnologia e Innovacion Productiva (Argentina – Observing run ID: GN-2003A-Q-53 and GN-2007B-Q-87.

† E-mail: demello@cua.edu

et al. 2008b) and outside the merger remnant NGC2782 (Torres-Flores et al. 2012).

The importance of these newly formed objects as products of collisions is still debatable. They may be responsible for enriching the intragroup medium with metals which may have broad implications for galaxy chemodynamical evolution (Werk et al. 2011). They could grow to become independent objects as dwarf galaxies, or live as stellar clusters in the distant halos of their hosts. In addition, one cannot exclude the possibility that they will dissolve and not remain gravitationally bound, yielding only very sparse star streams, or fall back onto the progenitor (Bournaud & Duc 2006).

UV images of tidal tails, obtained with the Galaxy Evolution Explorer (*GALEX*) satellite, showed UV-bright regions coincident with HI density enhancements (Hibbard et al. 2005, Neff et al. 2005). More recently, Thilker et al. (2009) reported the discovery of massive star formation in the Leo primordial HI ring which is having one of its first bursts of star formation. Therefore, UV and HI data together provide a powerful technique for identifying and studying star forming regions in the vicinity of interacting galaxies. In de Mello et al. (2008a) we presented a sample of 16 star forming region candidates in the intergalactic medium surrounding HCG 100. Here we present the optical data obtained with Gemini for HCG 100 and also for another compact group, HCG 92. We also present the UV data of six interacting galaxies with HI tails where we discovered 35 stellar cluster candidates.

This paper is organized as follows: §2 presents the data and results for HCG 92 and 100; §3 presents the comparison sample and the discussion; §4 presents the Summary, and the Appendix describes the comparison sample in more detail. Throughout the paper we assumed $\Omega_M = 0.3$, $\Omega_\Lambda = 0.7$, and $H_0 = 100$ h km s^{-1} Mpc^{-1}, with h=0.71.

2 HCG 92 AND HCG 100

The targets analyzed here are newly identified members of two Hickson compact groups of galaxies, HCG 92 and HCG 100 (Hickson 1982) located within their HI tails. HCG 92, known as Stephan's quintet (e.g. Moles et al. 1997, Sulentic et al. 2001, Gallagher et al. 2001), is formed by three late-type galaxies (NGC 7318a, 7318b, 7319), one early-type (NGC 7317) at 80 Mpc and one object, NGC 7320, which is a foreground object. Mendes de Oliveira et al. (2004) presented the discovery of four intergalactic HII regions in the HI tail of HCG 92 located more than 25 kpc from the nearest group galaxy.

HCG 100 is formed by a bright central Sb galaxy (HCG 100a), an irregular galaxy with an optical tidal tail (HCG 100b), a late-type barred spiral (HCG 100c) and a late-type edge-on spiral (HCG 100d). It is the last group of Hickson's catalog (1982) and is at 76.3 Mpc (v_R=5,336 km/s). de Mello et al. (2008a) presented GALEX FUV and NUV images of this group and identified 15 FUV sources located in the vicinity of the intergalactic HI clouds of the compact group which extends to over 130 kpc away from the main galaxies.

2.1 Spectroscopy with Gemini/GMOS

We have obtained new spectra of dozens of UV sources identified within the HI tails of HCG 92 and HCG 100 and derived their radial velocities. We also determined metallicities for those which turned out to be at the same redshift of the groups. Observations were performed with the Gemini Multiobject Spectrograph (GMOS) at Gemini North in June 2003 (HCG 92) and in October and November 2007 (HCG 100). We centered GMOS slit on members of the groups and on sources which were identified in Mendes de Oliveira et al. (2004) and de Mello et al. (2008a). Other objects in the field were also observed when there was space left in the multislit mask. The spectra were acquired using the B600 and R400 gratings.

Exposure times for HCG 92 were 3×1500 sec for the B600 granting and 3×1000 sec for the R400 grating, covering from 3700 to 8000 Å. For HCG 100 data, the total exposure times were 3×600 sec and 3×1200 sec for the B600 and R400 gratings, respectively, and the final spectra covered a wavelength interval of 3700 to 7000 Å. Position angles were 20 and 300 degrees, from the usual orientation of GMOS, values for the airmass were 1.22 (R400) and 1.08 (B600) for HCG 92 and 1.03 for HCG 100, respectively. The seeing of 1 arcsec matched well the slit size of 1 arcsec in both cases.

All spectra were biased, trimmed, flat fielded, and wavelength calibrated with the Gemini IRAF package version 1.8 inside IRAF[1]. The final spectra have typical resolutions of 3.2 and 7.0 Å for B600 and R400 gratings, respectively. The spectra of the regions in HCG 92 were not flux calibrated given that there were no standard calibrators observed around the time the data were taken. While the regions of HCG 100 had their flux calibrated using the spectrum of the stars BD+284211 (R400) and Hiltner 600 (B 600), observed in December 11, 2007. For reddening correction we used the intrinsic Hα/Hβ ratio, with an intrinsic value taken by Osterbrock (2006) for an effective temperature of 10000K and N_e=10^2.

We found 12 and 2 sources at the same redshift of HCG 92 and HCG 100, respectively. Four of the 12 sources had already been confirmed as members of HCG 92 by Mendes de Oliveira et al. (2004).

2.2 GALEX data

We obtained GALEX FUV and NUV background subtracted images from the Multimission Archive at the Space Telescope Science Institute (MAST) and followed the method by de Mello et. al (2008a) to select UV sources within the HI tail or in the outskirts of the HI map. FUV and NUV fluxes were calculated using Morrissey et al. (2005) m_λ=-2.5log[F_λ/a_λ] + b_λ. Fluxes were multiplied by the effective filter bandpass (FUV= 1528 ± 269 Å and NUV = 2271 ± 616 Å) to give units of erg s^{-1} cm^{-2}.

The GALEX fields of view are 1°.28 and 1°.24 in FUV and NUV, respectively, and the pixel scale is 1.5 arcsec pixel^{-1}. The images have a resolution (FWHM) of 4.2″and

[1] IRAF is distributed by the National Optical Astronomy Observatories, which are operated by the Association of Universities of Research in Astronomy, Inc., under cooperative agreement with the National Science Foundation.

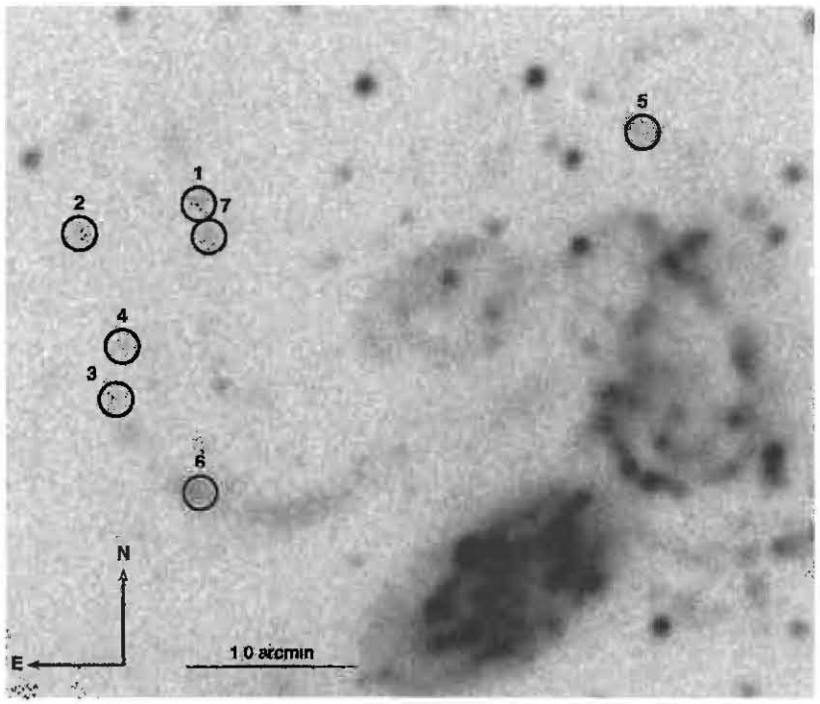

Figure 1. NUV image of HCG 92. Seven UV sources detected in the GALEX images are marked. North is up and East is to the left. Bar length is 1′.

5.3″ in FUV and NUV, respectively. Despite the broad FWHM, GALEX is able to detect faint UV sources. The medium imaging survey, for instance, reaches m=24 and 24.5 in FUV and NUV with typical exposures of 1,500s (Bianchi et al. 2007). GALEX images have also been used extensively to search for very low surface brightness objects (e. g. Thilker et al. 2007) such as the ones we are interested in detecting. We chose the parameters to detect the UV with Source Extractor and perform photometry (version 2.4.3, Bertin & Arnouts 1996, hereafter SE) following the prescription of de Mello et al. (2008a, 2008b) which was fine tuned for detecting low surface brightness objects and clumpy systems. We matched both catalogs, FUV and NUV, within 3″-4″ radius. The SE's UV magnitudes (Mag_auto, AB system) were corrected for foreground Galactic extinction using E(B − V) obtained from Schlegel et al. (1998) and A_{FUV} = E(B − V) × 8.29, and A_{NUV} = E(B − V) × 8.18 (Seibert et al. 2005). We used the Cortese et al. (2008) method for computing the internal extinction for each object in the FUV band. For each A_{FUV}, we used Seibert et al.

(2005) extinction law, shown above, to obtain the E(B-V).[2]

FUV and NUV colors were estimated using the task PHOT in IRAF, inside a fixed aperture of 4″ or 5″ radius, depending on the sizes of the sources, centered on the centroid of the light distribution of each NUV band detection.

2.3 Ages, masses and metallicities

We used the method described in de Mello et al. (2008a, 2008b) to derive ages and masses from FUV and NUV GALEX images (Table 1). For each region, ages were estimated using the models given by Starburst99 (SB99, Leitherer et al. 1999). These models were generated for an instantaneous burst, solar metallicity, Chabrier (2003) IMF, and are optimized for GALEX filters transmission curves. We have also generated models using Salpeter IMF and compared the results with Chabrier IMF. The difference in age between the two IMFs is around $\sim$ 2-4 Myr. In this paper we are presenting only the results generated with Chabrier IMF. We have also included in Table 1 the errors for each age calculated from the errors in the colors.

We compared the ages determined spectroscopically by Mendes de Oliveira et al. (2004) with our values using GALEX and found an excellent agreement for 3 of the 4 regions (#1,# 2 and #4) for HCG 92. The object for which our age determination disagrees with respect to Mendes de Oliveira et al. (their region C and our region 7) is too close to another object and GALEX is not able to resolve them. We have also estimated ages from the Hα equivalent widths and SB99 models (Table 1) and found agreement between the methods for 4 sources in HCG 92 and the 2 sources in HCG 100. However, 3 sources in HCG 92 are much older when calculated using the UV data than when using Hα. This could be due to the fact that ultraviolet light probes older stellar population than Hα and/or due to other factors including wrong correction for dust attenuation and positioning of the slit. We will discuss this later in this session when we compare our estimates with other authors. We cannot exclude the possibility that density bounded conditions could produce lower equivalent widths, that leading to apparent older ages when derived from them and SB99.

UV images showing the location of the newly detected members of HCG 92 and of HCG 100 are shown in Fig. 1 and 2. The Gemini optical image (r filter; Fig.3) shows the peculiar and knotty morphology of the two UV sources in HCG 100 which resemble dwarf galaxies. They are located in the HI tail and we suggest that they might be TDG candidates.

In Fig. 4 we show spectra taken with gratings R400 and B600 for the two TDG candidates of HCG 100, and in Fig.5-6 we present two new star-forming regions of HCG 92, regions 3 and 5, which are similar to the four objects described in Mendes de Oliveira et al. (2004).

Metallicities of the regions were calculated using the empirical methods O3N2 and N2, proposed and calibrated by Pettini and Pagel (2004). These methods use line ratios [OIII] λ5007/Hβ plus [NII] λ6584/Hα and [NII] λ6584/Hα, respectively, to estimate oxygen abundances. These estimators are adequate for faint extragalactic sources, such as the ones we are dealing with, because they are based only on very bright lines. The uncertainties on the calibration of these methods are 0.14 dex for O3N2 and 0.18 for N2 when 68% of the points are included. Table 1 shows the estimated metallicities for the regions in HCG 92 and HCG 100, plus our new results on velocities (measured from the emission lines), masses, and ages. As it can be noted in Table 1, the metallicities derived from the O3N2 and the N2 methods are in close agreement. For one of the regions of HCG 92 (region 6), we used only the N2 method due to the lack of Hβ.

We calculated line ratios and verified that all sources are star forming regions as shown in the BPT diagnostic diagram (Baldwin, Phillip &Terlevich 1981) in Fig.7. We plotted all Sloan sources from Kauffmann et al. (2003) for comparison.

In Fig.8 we show our new data plotted on the metallicity-luminosity diagram (adapted from Fig. 3 of Weilbacher et al. 2003). We estimated oxygen abundances using the method O3N2 described above. We also added new data from Croxall et al. (2009) to this figure. As expected, HCG 100 main members occupy the left side of the diagram where luminous and metal-rich objects are located. Nearby dwarf irregular galaxies (Richer & McCall 1995) follow the well-known correlation indicated by the linear fit. Based on Fig.8, all star-forming regions in the HI tail of HCG 92 and HCG 100 have metallicities similar to those of knots in tidal features, i.e. they have metallicities higher than those of local dwarf galaxies. Lisenfeld et al. (2008) and Mendes de Oliveira et al. (2004) found similar results for star-forming regions in the intergalactic medium of the systems Arp 94 and HCG 92, respectively.

Thus we conclude that the metallicity measurements obtained here allowed us to distinguish between "classical" dwarf galaxies and objects from tidal origin. We conclude that objects found within the HI tails of HCG 92 and HCG 100 were formed by pre-enriched material, and their metallicities are similar or higher to that of their progenitor galaxies. It is also possible that their higher metallicities are due to a phenomenon called Infant Mortality (Fall et al. 2005) which destroys clusters by internal processes. In this way, the continuous star formation and destruction of stellar clusters could increase the metallicity of a given region after a few million years.

We have compared the coordinates of our targets with the ones identified in Trancho et al. (2012) using Hubble Space Telescope images and Gemini spectroscopy of HCG 92 and found no common sources. However, a close inspection of the HST images indicate that object T124 in Trancho et al. is the same as our object #6, but had wrong coordinates quoted in their paper. The HI tail is twice as long and has a different curvature than the optical tail, therefore HST small field of view did not cover the entire HI tail. The work by

[2] The values we find for E(B-V) obtained from spectroscopy for regions 3 and 4 of HCG 100 are slightly different from the values calculated from the UV images. This difference could be due to the fact that the slit is not sampling the entire region and might be missing some of the regions where the UV flux originates. E(B-V) values are: Region 3 (0.10+-0.01, 0.13) and Region 4 (0.09+-0.02, 0.05) - first value is from imaging, second value is from spectroscopy.

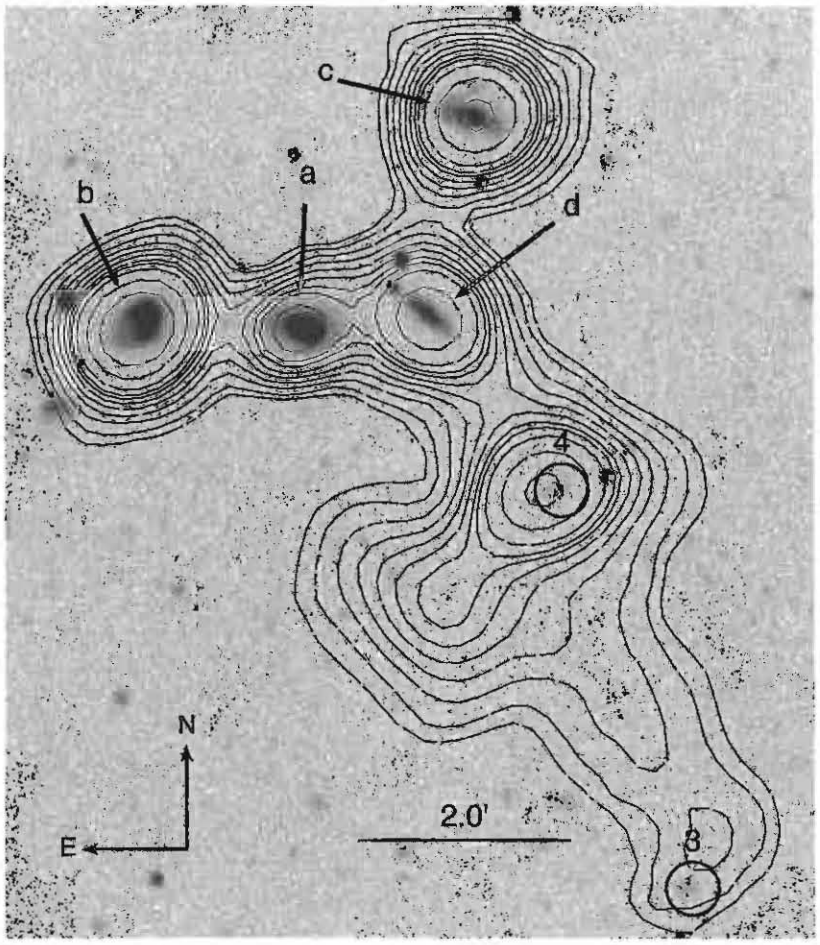

Figure 2. NUV image of HCG 100 where galaxy members a, b, c and d are labeled. Two TDG candidates, #3 and #4, are marked. They fall within the HI tail as shown in de Mello et al. (2008a). North is up and East is to the left. Bar length is 2′. VLA NHI contours are 0.6, 1.2, 2.1, 3.6, 4.4, 5.1, 5.9, 6.6, 7.4×10^{20} cm^{-2}.

Trancho et al. (see also Fedotov et al. 2012) focused only on the optical tail, missing most of the targets we discovered. The age reported by those authors for T124 is in relative good agreement with the values we found for object #6 using the Gemini spectra (1.5 Myr and 6 Myr, respectively). However, the age we found using the UV data, ∼100 Myr, is significantly higher. This disagreement can be explained, as pointed out in Trancho et al., by the fact that the slit did not cover the entire complex and is missing the other components of the clump. The UV data on the other hand covers the entire region and is more representative of the cluster. The UV is also known for detecting older stellar population than Hα and is a good age indicator for this type of stellar clusters. Therefore, our results suggest that T124 (or #6) is ∼100 Myr and $10^{8.5}$ $M_\odot$, making it the most massive TDG candidate in the outskirts of HCG 92. We have also inspected the location of this object with respect to the HI map (Mendes de Oliveira et al. 2004) and verified that it is located within one of density peaks which supports the idea that T124 (or #6) is a TDG candidate. According to Tran-

Table 1. Star-forming regions in the HI tail of HCG 92 and HCG 100

ID	ID_region	R.A. 2000	DEC. 2000	V (km s^{-1})	M_B[c] mag	12+log(O/H) O3N2	12+log(O/H) N2	Log($M_\star$)[b] $M_\odot$	Age[c] Myr	L_{FUV} erg s^{-1}
HCG 92	1[d]	339.04583	33.98667	6615 ± 16	-12.30	8.44±0.14	8.48±0.18	4.2	$2.1\pm\frac{1}{2}$[5.4]	40.74
	2[d]	339.06250	33.98417	6613 ± 59	-11.90	8.35±0.14	8.45±0.18	4.3	$2.2\pm\frac{2}{5}$[4.1]	40.71
	3	339.05833	33.96750	6577 ± 69	-11.58	8.45±0.14	8.55±0.18	4.1	$2.4\pm\frac{2}{5}$[5.5]	40.52
	4[d]	339.05833	33.97306	6659 ± 55	-12.10	8.48±0.14	8.57±0.18	5.7	$12.9\pm\frac{3}{5}$[5.5]	40.50
	5	339.99583	33.99417	6035 ± 19	-11.34	8.40±0.14	8.44±0.18	7.6	$50.1\pm\frac{1}{9}$[5.4]	41.30
	6	339.04583	33.95833	6543 ± 36	-12.57	...	8.69±0.18	8.5	$100\pm\frac{9}{3}$[6.4]	41.67
	7[d]	339.04583	33.98361	6612 ± 59	-12.69	8.32±0.14	8.38±0.18	7.9	$100\pm\frac{2}{4}$[2.44]	41.06
	8	339.07500	33.99333	5628 ± 17	-13.23	8.50±0.14	8.60±0.18	...	...[7.6]	...
	9	338.97500	33.95389	5780 ± 12	-14.10	8.36±0.14	8.48±0.18	...	...[3.4]	...
	10	338.98750	33.97972	6020 ± 81	-15.25	8.62±0.14	8.67±0.18	...	...[5.3]	...
	11	339.04583	33.98278	6553 ± 52	-12.07	8.36±0.14	8.47±0.18	...	...[5.6]	...
	12	339.04583	33.97389	6621 ± 71	-9.88	8.46±0.14	8.55±0.18	...	...[3.9]	...
HCG 100	3[e]	0.27083	13.02333	5440 ± 61	-14.54	8.43±0.14	8.43±0.18	4.7	$1.0\pm\frac{}{}$[6.1]	40.46
	4[e]	0.29167	13.08583	5337 ± 27	-13.42	8.42±0.14	8.55±0.18	4.7	$3.3\pm\frac{3}{1}$[2.1]	40.51

[a] Calculated using magnitudes from Mendes de Oliveira et al. (2004) and de Mello et al. (2008a).

[b] Stellar mass ($M_\odot$) obtained from Starburst99 monochromatic luminosity, L_{1530} (erg/s/Å), for the ages given in column 9. Stellar mass ($M_\odot$) for H100-#3 and H100-#4 are from de Mello et al. (2008).

[c] Age (Myr) estimated from FUV-NUV color. Values given in brackets: ages estimated from Hα equivalent width and SB99 models.

[d] The respective ID's in Mendes de Oliveira et al. (2004) for regions 1,2, 4, and 7 in this table are d, a, b, and c.

[e] ID from de Mello et al. (2008a).

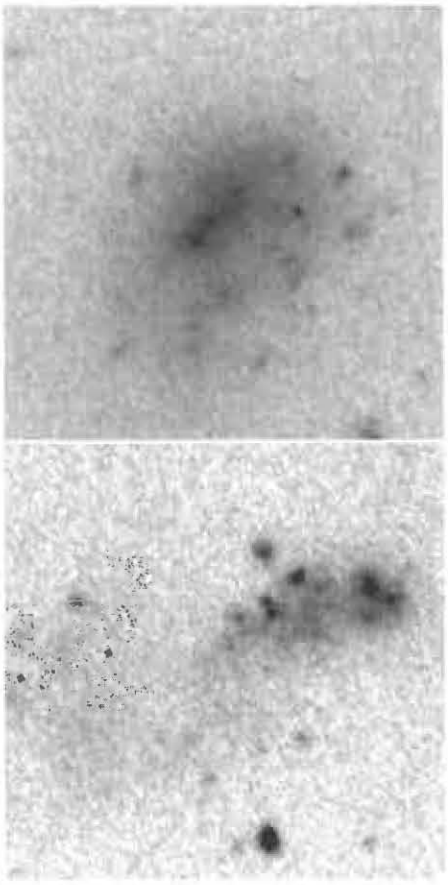

Figure 3. Gemini image (filter r) of the two TDG candidates in the HI tail of HCG 100 as originally identified in de Mello et al. (2008a) as objects #3 (top) and #4 (bottom). North is up and East is to the left.

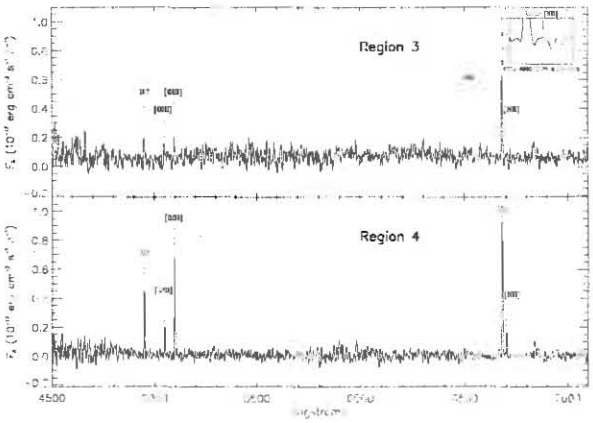

Figure 4. Spectra of HCG 100's regions 3 (top) and 4 (bottom) identified in de Mello et al. (2008a). These spectra were taken with B600 and R400 gratings. The marked lines were used to estimate the oxygen abundance (12+log(O/H)). A zoom into the Hα line region is shown on the right side of the top figure.

cho et al., two other stellar clusters close to T124, T117 and T122, are 7 and 50 Myr but are not resolved in the GALEX image and therefore are not part of our analysis. Another object, T118, is 125 Myr and has not passed our selection criteria (more details are given in the discussion Section 3). These 4 stellar clusters are within the optical tail which is estimated to have formed due to a close interaction between NGC 7318A and NGC 7319 ~ 200 Myr ago (Renaud et al. 2010). Therefore, our data show that HI tails in these two compact groups, HCG 92 and HCG 100, are laboratories of star formation.

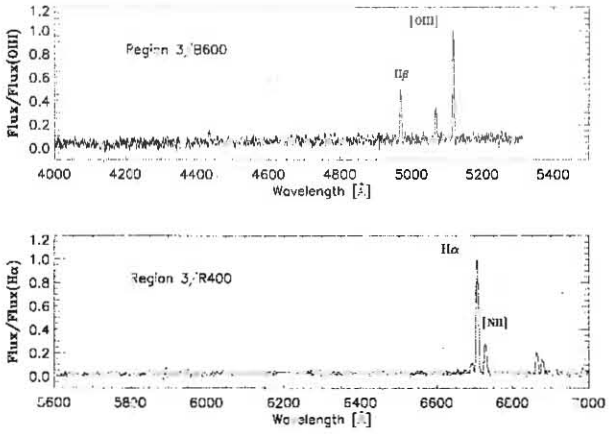

Figure 5. Spectra of HCG 92's region 3. Spectra taken with B600 grating is in the top panel and R400 is in the bottom one. The marked lines were used to estimate the metallicities (12+log(O/H)). These spectra were not flux calibrated, given that no calibration star was available.

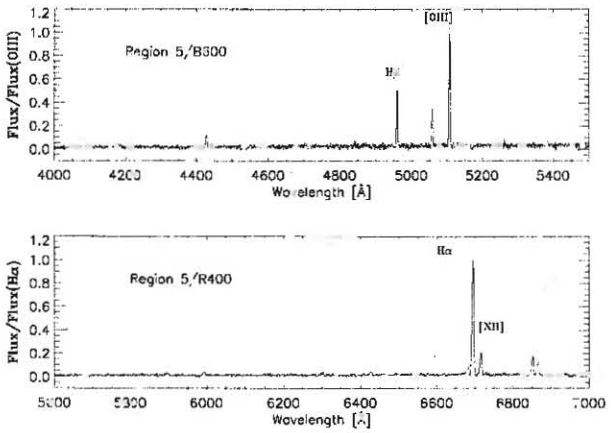

Figure 6. Spectra of HCG 92's region 5. Spectra taken with B600 grating is in the top panel and R400 are in the bottom one. The marked lines were used to estimate the metallicities (12+log(O/H)). These spectra were not flux calibrated, given that no calibration star was available.

3 DISCUSSION

In order to explore whether the environment where the newly discovered stellar clusters and TDG candidates plays a significant role in their formation, we have analyzed other interacting systems with extended HI tails using a sample of galaxies from the Rogues gallery of HI maps of peculiar and interacting galaxies compiled by J. Hibbard et al. (2001)[1]. We identified 25 interacting systems with GALEX data with exposure times > 1 ksec which have also been observed by the Sloan Digital Sky Survey (SDSS). We followed the same method to identify UV sources and to obtain their ages as we did for the compact groups. Since we are looking for young

[1] http://www.nrao.edu/astrores/HIrogues/RoguesLiving.shtml

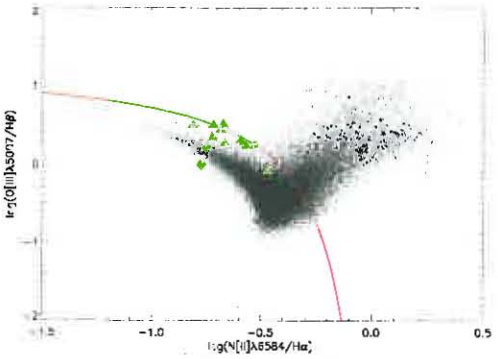

Figure 7. Line ratio diagram showing Sloan data from Kauffmann et al. (2003) and from star-forming regions in the HI tails of HCG 92 (triangles) and HCG 100 (diamonds). Objects with line ratios below the red line are classified as HII regions.

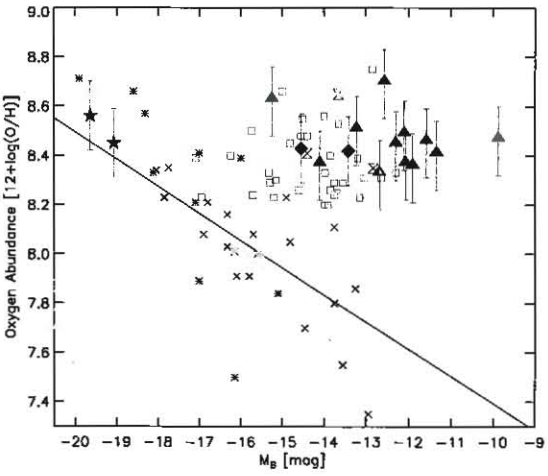

Figure 8. Absolute Magnitude (M_B) versus Oxygen Abundance for local isolated dwarf galaxies (crosses), knots in tidal features (open squares), main group members (asterisk), main members HCG 100 (stars), HII region of Croxall et al. (2009, Hourglass), and our TDG candidates from HCG 92 (filled triangles) and HCG 100 (filled diamond). The line shows the correlation for dwarf galaxies from Weilbacher et al. (2003). The metallicities were obtained with O3N2 index for the majority of the regions. N2 calibrator was obtained for only one region of HCG 92. Adapted from Weilbacher et al. (2003).

regions predominately composed by the luminosity of O, B, and A stars, we defined a conservative cut in age at 100 Myr. We note that all new objects reported in the previous session for HCG 92 and HCG 100 are within this age range. We have also adopted a cut in luminosity equivalent to 100 O 8V stars ($100 \times L_{FUV} = 100 \times 2 \times 10^{37}$ erg s^{-1}) or 4.2 $\times$ 10^{39} erg s^{-1}. This limit was set based on the luminosities of stellar clusters found in the HI bridge of M81 and M82 (a.k.a. "blue blobs") from de Mello et al. (2008b).

Six of the 25 interacting systems originally selected have 35 UV sources with ages < 100 Myr and luminosity higher than 4.2 $\times$ 10^{39} erg s^{-1} inside the HI contours. A description of each these six interacting systems is given in the

Appendix. In Table 2 we list the regions, their colors, ages, and luminosities, assuming that they are at the distance of the parent galaxies. Figs. 10 to 15 show the different systems with their HI contours and the marked UV sources. We cannot exclude the possibility that a few or various of the UV sources we selected might be unrelated to the interacting galaxies, i.e. might be chance alignments. However, this method, when applied to HCG 100 by de Mello et al. (2008a), selected two TDG candidates within the HI tail and several stellar clusters in M81/M82 (blue blobs, de Mello et al. 2008b). As shown in the previous session, our Gemini MOS data reveal that these two TDG candidates are at the same redshift as the galaxy group. Therefore, these two multi-wavelength studies show that this approach is successful in identifying UV sources which are either star-forming regions or TDGs related to the interacting systems with stripped HI gas.

In order to compare the properties of the 35 UV sources found outside interacting galaxies with ones in HCG 92 and HCG 100 we have calculated their luminosities and searched for similarities in the two populations. In Fig.9 we show the distribution of luminosities versus ages for the 35 regions and we verify that the population of intergalactic regions contains objects with luminosities as high as $\sim 10^{42}$ erg s^{-1} and as low as $\sim 10^{39}$ erg s^{-1}, our lower limit. It is possible that the large range in luminosities indicates that we are dealing with different families of objects, as suggested in Mendes de Oliveira et al. (2004). As seen in Fig.9 most of the regions in our sample are not as luminous as TDG candidates found in compact groups (filled symbols), except for object 2 around NGC 3079 and object 1 around NGC 3719. If that is the case, interacting galaxies are more likely to host star clusters while compact groups are more likely to host TDGs, as can be seen in Fig.9. The low mass objects might be similar to the M81-M82 "blue blobs" described above. The high mass objects would then be the TDG candidates. The Kolmogorov-Smirnov probability test confirms that luminosities of stellar clusters in interacting systems are significantly different from the ones in compact groups (KS = 0.00013), i.e. luminosities are lower in the former than in the latter. We have also calculated masses using Starburst99 (Column 8 in Table2) and the same trend is verified.

Further spectroscopic observations of these regions, as we did for HCG 92 and HCG 100, are needed in order to confirm their membership and establish their metallicities. It is possible that the group environment is more conducive to TDG formation (or better said, TDG survival) than pairs and mergers. This is in agreement with the simulations by Bournaud & Duc (2006) where specific conditions such as low impact velocity (v< 250 km s^{-1}), prograde encounters and mass ratio up to 4:1 may lead to TDG formation. HCGs might harbor these conditions besides the possibility that group potential may be able to drive TDGs away from the nearby proximity of their progenitor galaxies.

4 SUMMARY

We presented new Gemini spectroscopy of fourteen star-forming regions within the HI tails of HCG 92 and in HCG 100 confirming that they are at same redshifts of the groups. We estimated their metallicity and verified that they

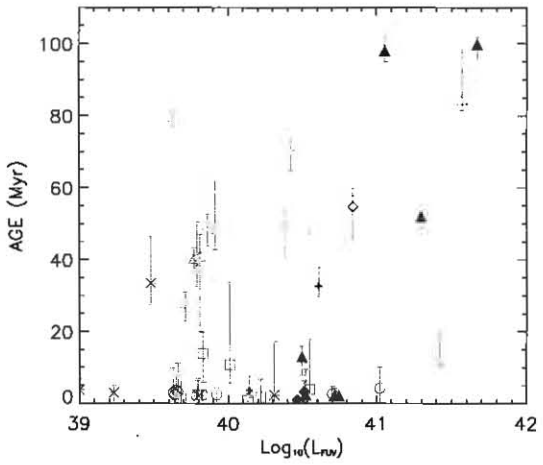

Figure 9. FUV luminosity (erg s^{-1}) versus age (Myr) for star-forming regions outside galaxies in 6 interacting galaxies (different symbol), HCG 100 (filled diamond) and HCG 92 (filled triangles).

are metal-rich with respect to typical dwarf galaxies. This is possibly due to the fact that they were formed from pre-enriched material found in the intragroup medium.

We analyzed GALEX FUV and NUV data of a comparison sample of 6 interacting galaxies containing a total of 35 UV sources in the HI tails. These star-forming regions span a wide range of ages (< 100Myr) and luminosity (10^{39} – 10^{42} erg s^{-1}). We compared their properties with those of the star-forming regions in the HI tails of HCG 92 and HCG 100. We concluded that they have on average lower luminosity than the ones in the HI tails of compact groups. We suggest that this maybe is an environmental effect, i.e. that compact groups of galaxies with tidal tails of HI are more likely to host more massive star-forming regions or TDGs than other interacting galaxies. Spectroscopy of these sources are needed in order to confirm that they are at the same redshift as the interacting galaxies and to establish their metallicities.

4.1 Appendix

We present the GALEX/FUV images of the 6 interacting systems with extended HI gas. The FUV sources with ages < 100 Myr and L> 10^{39} erg s^{-1} are marked. The HI contours are adapted from Hibbard et al. (2001).

4.1.1 NGC 2623

NGC 2623, also known as Arp 243, is located at 76.1 Mpc (Hattori et al. 2004). Bournaud et al. (2004) and Hattori et al. (2004) classified this object as a merger in an advanced stage. Hibbard & Yun (1996) found that a large part of the HI gas is located far away from the stellar component of NGC 2623.

In our analysis we detected two young UV sources in the western tail of NGC 2623, as show in Fig. 10. One of them (region #1 in Figure 5) seems to be associated with the giant HII region (which could be a TDG candidate)

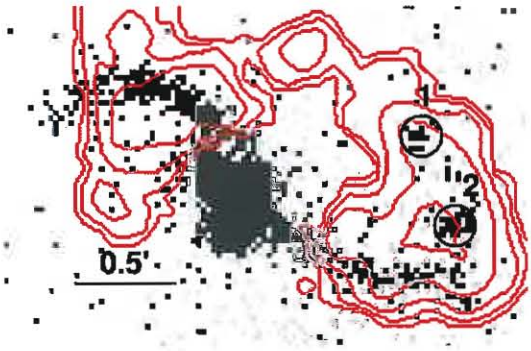

Figure 10. FUV image of NGC 2623, regions with ages < 100 Myr are marked with circles of 6" radius. HI contours=4 $\times 10^{19}$cm$^{-2}\times 2^n$ are from VLA C+D-array and provided by Hibbard et al. (2001).

detected by Bournaud et al. (2004) in their Fabry- Perot study. The age of this region is only 3 Myr. Its mass is about five times the mean mass of the intergalactic HII regions of Mendes de Oliveira et al. (2004). We detect another young region, #2 (Figure 10), within the HI contours of NGC 2623. Interestingly, this region is also detected in the Hα map shown in Bournaud et al. (2004). The detection in the narrow band image confirms that these two regions belong to the NGC 2623 system. In Table 2 we list the main physical parameters for each object.

4.1.2 NGC 3079

NGC 3079 is a giant spiral galaxy with two companions, MCG 9-17-9 (northeast) and NGC 3073 (southeast). NGC 3079 is located at 15 Mpc (de Vaucoulers et al. 1991) and it is a Seyfert 2/LINER with X-ray emission (Irwin & Saikia 2003; Kondratko et al. 2005). This galaxy is one of the brightest observed mergers (Henkel et al. 1984). NGC 3073 is a dwarf galaxy with an elongated HI tail aligned with the core of NGC 3079.

We found six UV sources (Fig. 11) in this system. One of them seems to be associated with the HI contours of NGC3073. In Table 2 we list the main physical parameters for each object. HI contours

4.1.3 NGC 3359

NGC 3359 is a barred spiral galaxy with several spiral arms and an irregular morphology in the outer parts of the disk.

NGC 3359 is at 13.4 Mpc (Rozas 2008) and it shows strong arms in the UV which are not observed in the optical. We detected 7 UV sources (Fig. 12) in this peculiar spiral, plus one UV source in the isolated HI cloud far from the disk (region 5).

4.1.4 NGC 3627

NGC 3627 is part of the Leo Triplet together with NGC 3623 and NGC 3628. The system is located at 6.7 Mpc (de Vaucouleurs 1975) and contain a remarkable HI bridge and tail which can be due to an encounter between the galaxies in the past.

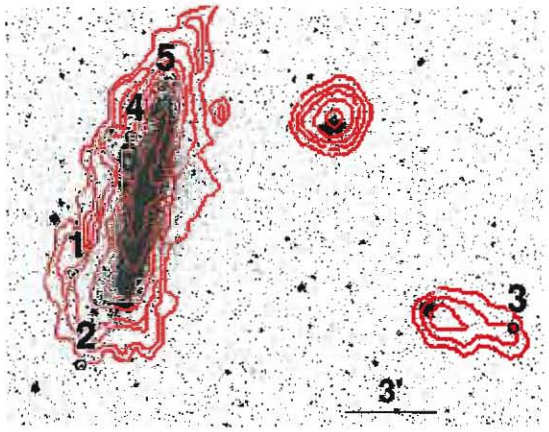

Figure 11. FUV image of NGC 3079, regions with ages < 100 Myr are marked with circles of 10" radius. NGC 3073 is a weak UV source close to source #3 in the figure. HI contours=(0.5, 1, 1.5, 2.4, 4, 10, 15, 25, 45) $\times 10^{20}$cm^{-2} are from VLA D-array and provided by Hibbard et al. (2001).

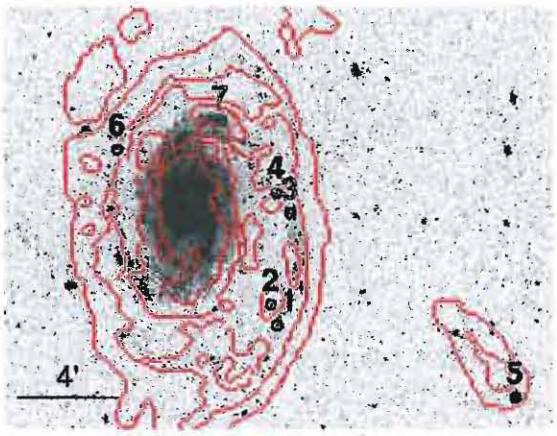

Figure 12. FUV image of NGC 3359, regions with ages < 100 Myr are marked with circles of 11" radius. HI contours=3 $\times 10^{19}$cm$^{-2}\times 2^n$ are from WSRT (30" resolution). The most outer contour is 5×10^{18}cm^{-2} for 60" resolution, and provided by Hibbard et al. (2001).

Here we present the results (Table 2) only for NGC 3627 (Fig. 13) since the other members are outside the GALEX field of view. We find only one UV source within the HI contour, located close to where HI seems to peak.

4.1.5 NGC 3718

NGC 3718 is part of the Great Bear group and it is at 17 Mpc (Tully 1998). This galaxy has a peculiar morphology, showing strong dust lanes and diffuse/peculiar spiral arms. It has a large extension of HI gas, far from the optical disk (Allsopp 1979).

NGC 3718 has 11 UV sources within the HI contour in both arms of the galaxy and outside the R_{25} optical radius (Fig. 14, Table 2).

Table 2. UV sources (ages < 100 Myr) in HI tails of 6 interacting galaxies

ID	ID_region	R.A.J2000	DEC.J2000	FUV-NUV[a]	Age Myr[b]	L_{FUV} (erg s^{-1})	Log($M_\odot$)[c]
NGC2623	1	129.5834808	25.7584667	-0.14 ± 0.16	$3.6\pm^{4}_{2}$	40.14	4.7
NGC2623	2	129.5805054	25.7511082	0.03 ± 0.11	$32.7\pm^{5}_{3}$	40.61	6.6
NGC3079	1	150.5596161	55.6378441	-0.43 ± 0.02	$1.0\pm^{1}_{1}$	40.52	4.3
NGC3079	2	150.5514526	55.5880432	-0.21 ± 0.12	$3.0\pm^{3}_{2}$	39.23	3.6
NGC3079	3	150.1344757	55.6083908	0.02 ± 0.04	$33.4\pm^{13}_{6}$	39.48	6.0
NGC3079	4	150.5026245	55.7128906	-0.19 ± 0.14	$3.7\pm^{5}_{3}$	39.95	3.8
NGC3079	5	150.4724426	55.7403946	-0.32 ± 0.13	$2.1\pm^{3}_{2}$	39.80	3.3
NGC3079	6	150.5094452	55.6856461	-0.22 ± 0.21	$2.3\pm^{15}_{5}$	40.31	3.8
NGC3359	1	161.5222015	63.1473923	-0.26 ± 0.21	$2.7\pm^{5}_{2}$	40.70	4.3
NGC3359	2	161.5304108	63.1609001	-0.13 ±0.20	$3.7\pm^{4}_{1}$	39.65	3.5
NGC3359	3	161.5033569	63.2215042	-0.30 ± 0.18	$2.4\pm^{5}_{2}$	39.92	3.5
NGC3359	4	161.5233002	63.2346001	-0.09 ± 0.17	$4.2\pm^{6}_{3}$	41.02	5.0
NGC3359	5	161.1769409	63.1001740	-0.23 ± 0.06	$2.9\pm^{2}_{2}$	39.63	3.2
NGC3359	6	161.7557220	63.2623863	-0.25 ± 0.2	$2.5\pm^{2}_{2}$	39.64	3.2
NGC3359	7	161.6039429	63.2815933	-0.16 ± 0.13	$3.3\pm^{3}_{2}$	39.66	3.4
NGC3627	1	170.1986084	12.9696226	0.67 ± 0.08	$0.1\pm^{0}_{0}$	41.43	5.2
NGC3718	1	173.2548523	53.1872864	0.14 ± 0.19	$84.5\pm^{14}_{3}$	41.57	7.2
NGC3718	2	173.2459717	53.1571503	0.05 ± 0.27	$49.7\pm^{3}_{6}$	39.86	5.8
NGC3718	3	173.2224731	53.1303406	-0.08 ± 0.06	$12.2\pm^{2}_{2}$	41.42	5.9
NGC3718	4	173.2071838	53.1464157	0.05 ± 0.13	$49.5\pm^{3}_{9}$	40.38	5.7
NGC3718	5	173.1886292	53.1595993	0.02 ± 0.12	$41.0\pm^{21}_{9}$	39.81	5.0
NGC3718	6	173.1446991	53.1508026	-0.02 ± 0.17	$30.0\pm^{3}_{5}$	39.71	4.6
NGC3718	7	173.0174866	53.1026154	0.11 ± 0.09	$71.8\pm^{5}_{7}$	40.42	6.0
NGC3718	8	173.0266724	52.9917526	0.02 ± 0.18	$40.3\pm^{3}_{3}$	39.76	4.9
NGC3718	9	173.1674805	52.9503860	0.13 ± 0.18	$79.9\pm^{1}_{4}$	39.62	5.3
NGC3718	10	173.2238617	53.0397415	0.01 ± 0.14	$37.5\pm^{13}_{3}$	39.79	4.9
NGC3718	11	173.0760498	53.0345230	0.05 ± 0.12	$48.7\pm^{14}_{6}$	39.91	5.2
NGC4656	1	191.0442352	32.2628098	-0.05 ± 0.20	$3.8\pm^{14}_{1}$	40.55	4.4
NGC4656	2	191.0705109	32.2710037	-0.09 ± 0.20	$10.8\pm^{23}_{5}$	40.01	5.1
NGC4656	3	191.0773621	32.2755814	-0.10 ± 0.18	$2.5\pm^{4}_{12}$	39.79	3.4
NGC4656	4	191.0822449	32.2876625	-0.24 ± 0.06	$1.8\pm^{5}_{15}$	40.22	3.7
NGC4656	5	191.0815887	32.2807884	-0.26 ± 0.22	$1.3\pm^{2}_{2}$	39.68	3.3
NGC4656	6	191.0652161	32.2919540	-0.07 ± 0.03	$13.8\pm^{6}_{8}$	39.83	5.1
NGC4656	7	191.0808105	32.3068008	-0.31 ± 0.14	$1.0\pm^{2}_{1}$	40.13	3.8
NGC4656	8	191.0811768	32.3120995	-0.09 ± 0.13	$2.5\pm^{1}_{6}$	39.82	3.4

[a] FUV and NUV magnitudes and errors were obtained using IRAF task phot (Poisson). The errors in the colors were calculated using the magnitude errors added in quadrature.

[b] Age (Myr) estimated from FUV-NUV color.

[c] Stellar mass ($M_\odot$) obtained from Starburst99 monochromatic luminosity, L_{1530} (erg/s/Å), for the ages given in column 6.

4.1.6 NGC 4656

NGC 4656 is a spiral galaxy (Sc) interacting with NGC 4631 (Roberts 1968). They are linked by an HI bridge and are at 7.5 Mpc (Hummel et al. 1984). The bright region to the North of NGC 4656 resembles a TDG in the process of formation. We detected 8 UV sources in this area (Fig. 15 and Table 2).

ACKNOWLEDGEMENTS

We are grateful to an anonymous referee for helpful comments and suggestions. DFdM was funded by NASA Research Grants NNG06GG45G and NNG06GG59G. F. U-V. acknowledges the financial support of FAPESP through an M. Sc. Fellowship, under contract 2007/06436-4 .C. M. d. O. acknowledges support from Brazilian agencies FAPESP (projeto temático 2006/56213-9), CNPq and CAPES. S. TF. acknowledges the financial support of FONDECYT (Chile) through a post-doctoral position, under contract 3110087 and FAPESP through the Doctoral position, under contract 2007/07973-3. This research has made use of the NASA/IPAC Extragalactic Database (NED) which is operated by the Jet Propulsion Laboratory, California Institute of Technology, under contract with the National Aeronautics and Space Administration. Some of the data presented in this paper were obtained from the Multimission Archive at the Space Telescope Science Institute (MAST). STScI is operated by the Association of Universities for Research in Astronomy, Inc., under NASA contract NAS5-26555. Support for MAST for non-HST data is provided by the NASA Office of Space Science via grant NAG5-7584 and by other grants and contracts.

REFERENCES

Allsopp, N.J. 1979, MNRAS, 186, 343
Baldwin, J.A., Phillips, M.M., & Terlevich, R., 1981, PASP, 93, 5
Bertin, E., & Arnouts, S. 1996, A&A S.S., 117, 393
Bianchi, L. 2007, ApJS, 173, 659
Bournaud F., Duc P.-A., Amram P, Combes F., Gach J.-L. 2004, A&A, 425, 813
Bournaud, F. & Duc, P.-A., 2006, A&A, 456, 481
Chabrier, G. 2003, PASP. 115, 763
Cortese, L., Boselli, A., Franzetti, P., et al. 2008, MNRAS, 386, 1157
Croxall, K., van Zee, L., Lee, H., et al. 2009, AJ, 705, 72
de Mello, D. F., Torres-Flores, S. & Mendes de Oliveira, C. 2008a, AJ, 135, 319
de Mello, D.F., Smith, L. J., Sabbi, E., Gallagher, J. S., Mountain, M. & Harbeck, D. R. 2008b, AJ, 135, 548
de Vaucouleurs, G. 1975, ApJ, 202, 319

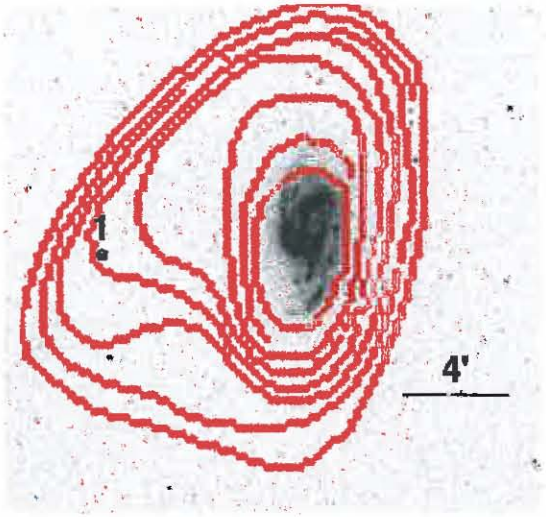

Figure 13. FUV image of NGC 3627, regions with ages < 100 Myr are marked with circles of 8" radius. HI contours= (3, 5, 10, 15, 25, 50, 75, 100, 200, 400, 600) K km s^{-1} are from Arecibo and provided by Hibbard et al. (2001).

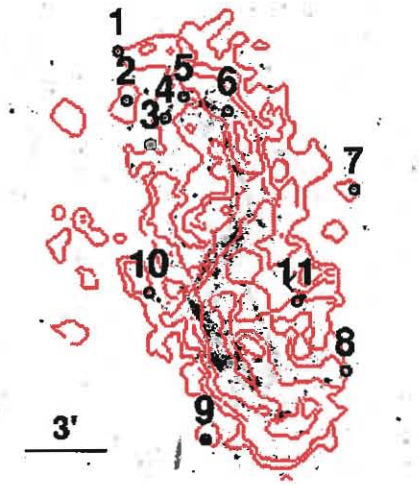

Figure 14. FUV image of NGC 3718, region with age < 100 Myr is marked with circle of 10" radius. HI contours =2 $\times 10^{20}$cm$^{-2}\times 2^n$ are from WSRT and provided by Hibbard et al. (2001).

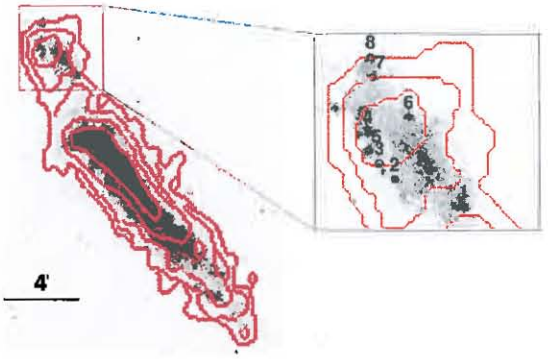

Figure 15. FUV image of NGC 4656, and a zoom of the candidate to TDG, the regions with ages < 100 Myr are marked with circles of 4" radius. HI contours =2 $\times 10^{19}$cm$^{-2}\times 2^n$ are from WSRT and provided by Hibbard et al. (2001).

de Vaucouleurs, G., et al. 1991, Third Reference Catalogue of Bright Galaxies (New York : Springer)

Fedotov et al. 2012. AJ accepted (arXiv:1105.5840v1)

Fall, S. M., Chandar, R., & Whitmore, B. C. 2005, ApJ, 631, L133

Gil de Paz, A., Boissier, S., Madore, B., et al. 2007, ApJS, 173, 185

Gallagher, S. C., Charlton, J. C., & Hunsberger, S. D. et al., 2001, AJ, 122, 163

Hattori T., Yoshida M., et al. 2004, AJ, 127, 736

Henkel C., Guesten R., Downes D., Thum C., Wilson T. L., Biermann P., 1984, A&A, 141, L1

Hibbard J., van Gorkom, J.H., Rupen, M.P, et al. 2001, ASP Conference Series, Vol. 240

Hibbard, J., Bianchi, L., Thilker, D., et al. 2005, ApJ, 619, L87

Hibbard, J., & Yun, M. 1996, Conference Cold Gas at High Redshift. eds. M.N. Bremer.

Hickson, P. 1982, AJ, 255, 382

Hickson, P. 1993, Astrophys.Lett. Comm., 29, 1

Hummel, E., Sancisi, R., & Ekers, R. D. 1984, A&A, 133,

Iglesias-Pramo, J. & Vlchez, J. M. 2001, 550, 204

Irwin J. A. & Saikia D. J. 2003, MNRAS, 346, 977

Kauffmann, G., Heckman, T.M., White, S.D.M., Charlot, S., Tremonti, C., et al. 2003, MNRAS 341, 54

Kondratko P., Greenhill L., Moran J. 2005, ApJ, 618, 618

Leitherer, C., Schaerer, D., Goldader, J., et al. 1999, ApJS, 123, 3

Lisenfeld, U. Mundell, C. G., Schinnerer, E., et al. 2008, AJ, 685, 181

Mendes de Oliveira, C., Cypriano, E.S., & Sodré,L. Jr, Balkowski, C. 2004, ApJ, L17

Mendes de Oliveira, C., Temporin S., Cypriano, E.S., Plana, H., Amram, P., & Sodré,L. Jr, Balkowski, C. 2006, AJ, 132, 570

Moles, M., Sulentic, J. W., & Marquez, I. 1997, ApJ 485, L69

Morrisey, P., Schiminovich, D., Barlow, T., et al. 2005, ApJ, 619, L7

Mullan, B., et al. 2011, ApJ 731, 93

Neff, S.G., Thilker, D., Sibert, M., et al. 2005, ApJ, 619, L91

Pettini, M. & Pagel, B. E. J., 2004, MNRAS, 348, L59

Oosterloo, R., et al. 2004 in 'Recycling Intergalactic and Interstellar Matter' IAUS 217. Eds., P-A Duc, J. Braine, & E. Brinks, 486, 492

Osterbrock, D., Ferland, G., 2006, "Astrophysics of Gaseous Nebulae and Active Galactic Nuclei"

Renaud, F., Appleton, P. N., & Xu, C. K. 2010, ApJ 724, 80

Richer, M. & McCall, M. 1995, ApJ 445. 642

Roberts, M.S. 1968, ApJ, 151, 117

Ryan-Weber, E.V., Meuerer,G.R., Freeman, K.C.,et al. 2004, AJ, 127, 1431

Schelegel, D.J., Finkbeiner, D.P., & Davis, M. 1998, ApJ 500, 525

Seibert, M., Martin, D., Heckman, T., et al. 2005, ApJ 619, L55

Sulentic, J. W., Rosado, M., Dultzin-Hacyan, D., Verdes-Montenegro, L., Trinchieri, G., Xu, C., & Pietsch, W. 2001, AJ 122, 293

Thilker, D., Donovan, J., Schiminovich, D., et al. 2009, Nature, 457, 990

Thilker et al. 2007, ApJS, 173, 538

Torres-Flores, S., Mendes de Oliveira, C., de Mello, D., et al. 2009, A&A 507, 723

Torres-Flores, Mendes de Oliveira, C., de Mello, D., et al. 2012, MNRAS, 421, 3612

Trancho, G., et al. 2012. submitted (arXiv:1201.5149v1)

Tully R. B. 1988, Nearby Galaxies Catalog (Cambridge: Cambridge Univ. Press)
Weilbacher, P. M., Fritze-v. A., Duc , P, et al. 2002, ApJ 579, L79
Weilbacher, P. M., Duc, P.-A., & Alvensleben, U. F-v. 2003, A&A 397, 545
Werk, J.K., et al. 2011, ApJ 678, 888